Проведено дослідження повздовжньо-динамічної навантаженості залізничного складу при встановленому русі по колії однорідного профілю. Визначено значення повздовжнього навантаження, яке діє на залізничний склад. При цьому розрахунки проведені для поїзда, що складається з 40 однотипних напіввагонів. Величина повздовжнього навантаження при цьому прийнята рівною 1,2 МН. Важливо зазначити, що при збільшенні швидкості руху, а також ваги поїзда, значення повздовжнього навантаження може перевищувати зазначену величину. Це сприяє додатковій навантаженості несучих конструкцій вагонів у складі поїзда і може стати причиною їх пошкоджень. Крім того, значні повздовжньо-динамічні навантаження сприяють порушенню стійкості руху вагонів у складі поїзда.

З метою зменшення повздовжньо-динамічних зусиль в поїзді при експлуатаційних режимах, в тому числі при гальмуванні, запропоновано використання замість типового автозчепного пристрою концепту упряжного пристрою. При цьому гасіння кінетичної енергії удару відбувається за рахунок перетворення її у роботу сил в'язкого опору. Цей опір створюється за рахунок переміщення через дросельні отвори поршня в'язкої рідини за принципом роботи гідравлічного демпфера.

Для обґрунтування використання концепту упряжного пристрою проведено розрахунок за методом визначення сили за зчіпним пристроєм шляхом уявного розділення поїзда на дві частини.

З урахуванням коефіцієнту в'язкого опору, що створюється концептом упряжного пристрою прискорення, яке діє на залізничний склад, склало близько 0,8 м/с^2. Тобто використання концепту упряжного пристрою дозволяє знизити повздовжню навантаженість поїзда майже на 30 % у порівнянні з типовою схемою взаємодії локомотива з вагонами.

Проведено розрахунок на міцність штоку концепту упряжного пристрою. Встановлено, що максимальні еквівалентні напруження не перевищують допустимі.

Запропоновані заходи сприятимуть зменшенню динамічної навантаженості залізничного складу при експлуатаційних режимах навантаження. Також впровадження даного концепту сприятиме зменшенню пошкоджень одиниць залізничного складу в експлуатації

Ключові слова: залізничний склад, повздовжня динаміка, динамічна навантаженість, концепт упряжного пристрою, моделювання динаміки

UDC 629.463.001.63
DOI: 10.15587/1729-4061.2020.198660

DEFINING PATTERNS IN THE LONGITUDINAL LOAD ON A TRAIN EQUIPPED WITH THE NEW CONCEPTUAL COUPLERS

O. Fomin
Doctor of Technical Sciences, Professor
Department of Cars and Carriage Facilities
State University of Infrastructure and Technologies
Kyrylivska str., 9, Kyiv, Ukraine, 04071

A. Lovska
PhD, Associate Professor
Department of Wagons*
E-mail: alyonaLovskaya.vagons@gmail.com

O. Kovtun
PhD
Department of General Technical Subjects
Danube Institute of the National University
"Odessa Maritime Academy"
Fanahoriyska str., 9, Izmail, Ukraine, 68601

V. Nerubatskyi
PhD, Associate Professor
Department of Electric Power Engineering,
Electrical Engineering and Electromechanics*
*Ukrainian State University of Railway Transport
Feierbakha sq., 7, Kharkiv, Ukraine, 61050

Received date 01.01.2020
Accepted date 06.03.2020
Published date 24.04.2020

1. Introduction

Ensuring the efficient operation of railroads as a leading sector of the transportation network requires the commissioning of modern rolling stock. In this case, making it more competitive predetermines the stricter requirements not only to the technical and economic indicators of rolling stock but also to the possibility of adapting the structures to the appropriate operating conditions.

It is known that one of the most loaded nodes in the design of rolling stock is automatic coupling equipment. During operation, this node experiences significant longitudinal-dynamic loads whose numerical values can be up to 3.5 MN – collision at shunting. In addition, significant loads emerge when operating the rolling stock on main tracks – braking, pulling off, etc.

To ensure that wagons are coupled to each other and to a locomotive, that they are kept at a certain distance from each other, and that the longitudinal efforts are transferred, the trains that include cars with a gauge of 1520 mm use the standard automatic coupling device SA-3 (Fig. 1). At present, there are the modernized variants of a given automatic coupler as well.

It is important to note that one of the main shortcomings of a given design is a significant cost, due to the use of a large number of components, specifically a coupler with the absorbing device.

This necessitates the implementation of new variants of automatic coupling devices. In this case, they should ensure the possibility to perceive and damp impact loads while meeting the conditions of strength for the rolling stock bearing structures. This would improve the operating efficiency of rolling stock and reduce the cost of unscheduled repairs.

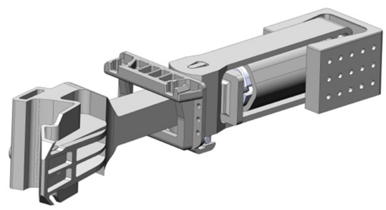

a

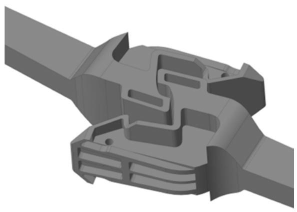

b

Fig. 1. Automatic coupling device SA-3:
a — automatic coupling design; *b* — car coupling

2. Literature review and problem statement

Paper [1] reports the results of mathematical modeling of train longitudinal dynamics. The authors gave the main theoretical positions, on the basis of which they developed an apparatus for determining the longitudinal efforts in a train. However, they failed to pay attention to devising measures to reduce the longitudinal efforts in a train.

The measures to improve the efficiency of rolling stock brakes operation were addressed in [2]. The author tested a graphic-analytical algorithm for the dual wear of the pads, which makes it possible to determine the magnitude and direction of the action of force factors. However, the author did not conduct research on the influence of these factors on the longitudinal dynamics of a train.

Work [3] studied the longitudinal-dynamic forces in a cargo train using different types of absorbing devices (Sh-1-T, Sh-2-T, and Sh-2-V). The longitudinal dynamics were simulated employing the software Universal Mechanism UM8.1. The authors analyzed the values of the longitudinal efforts in a train and defined the type of absorbing device that is the most optimal one to use.

The issue of improvement of the design of an automatic coupling device in order to reduce the longitudinal loading on cars in a train was not considered in the cited work.

The influence of the length of a train on the longitudinal forces at braking is examined in [4]. The study was conducted in the programming environment MATLAB. Based on their calculations, the authors found the longitudinal loads that act on the train composed of a different number of cars. However, no measures to reduce the longitudinal loads were proposed.

Paper [5] determined the longitudinal dynamics in the coupled trains. Wireless measuring equipment was developed, which allowed the authors to find indicators for the longitudinal dynamics of a train. However, they did not consider the task of determining the longitudinal loads in a train by mathematical modeling.

The distribution of the longitudinal-dynamic forces for various characteristics of the hysteretic buffer was reported in [6]. The paper takes into consideration that the time of filling the brake cylinders with compressed air and the parameters of the car buffers in a passenger train are the same. That is, the cars have the same braking force.

The development of the longitudinal-dynamic forces in a passenger train at braking is examined in [7]. The authors considered the influence of the number of cars in a train, the gross weight, and a deviation of ±20 % for length on the braking force.

However, the authors of [6, 7] did not consider the issue of distribution and reduction of the longitudinal-dynamic forces in cargo trains.

Work [8] analyzed the longitudinal dynamics of a train under operating modes. In this case, the longitudinal dynamics and the coupling force were modeled according to the results of experimental research. The model was solved in the MATLAB software suite. The cited work did not consider the improvement of the design of devices that couple cars and a locomotive to reduce the longitudinal-dynamic load on a train.

The simulation of vehicle dynamics under loading operating regimes is reported in [9]. The calculations were conducted in the Universal Mechanism programming environment. The authors took into consideration the different microgeometry of the track. The maximal values of the longitudinal efforts in a train were derived. However, no measures to reduce the longitudinal forces in a train during operating modes were proposed in the cited work.

The evolution of the simulation of longitudinal train dynamics was considered in [10]. The authors defined a series of potential research topics regarding the longitudinal dynamics of trains, which should be solved at the present stage of the development of the railroad industry in order to ensure the safety of motion. However, the issues of improving the coupling devices in order to reduce the longitudinal efforts in a train were not considered.

Our analysis of literary sources makes it possible to conclude that it is expedient to conduct research aimed at determining the longitudinal dynamics of a railroad train. A feature of this research is that the units of rolling stock interact between themselves through the new conceptual coupler. This would reduce the longitudinal loading on a train during operating modes.

3. The aim and objectives of the study

The aim of this study is to determine patterns in the longitudinal loading on the rolling stock taking into consideration the application of the new conceptual couplers instead of the automatic coupling of the SA-3 type.

To accomplish the aim, the following tasks have been set:

– to simulate the longitudinal load on a railroad train equipped with the new conceptual couplers;

– to estimate the strength of the rod of the conceptual coupler.

4. Methods for determining the longitudinal load on a train at steady motion

It is known that the maximal longitudinal effort at steady motion along a track of a uniform profile emerges in an automatic coupling device between a locomotive and the train's cars (Fig. 2). The features of determining the longitudinal efforts in a train are described in [11].

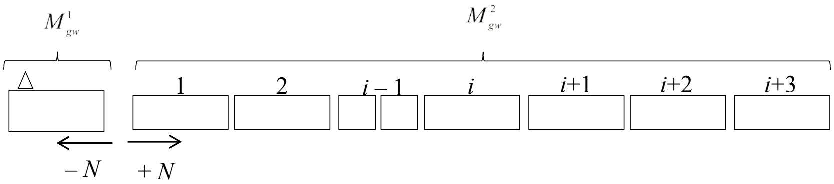

Fig. 2. Estimated scheme of a train: M^1_{gw}, M^2_{gw} are, respectively, the gross weight of the left and right parts of the train

In addition, the longitudinal effort in a train can be derived using the procedure given in [12]:

$$N=\left[\frac{T_k}{Q_0+Q}-w_{cp}-b_T\right]\cdot Q+\sum_{i=1}^{n}\left(Q_i\cdot w_i+B_{T_i}\right), \tag{1}$$

where T_k is the tangent traction force of a locomotive, kN; Q_i is the weight of a unit of a train with serial number i, forward direction (at i=0 – the main locomotive, i=1, 2, 3,..., n – cars), kN; w_{cp}, b_T are, respectively, the average resistance and average braking force per unit weight of the train, kN; n is the number of cars in the train; w_i is the specific motion resistance of a rolling stock unit, taking into consideration the track profile; B_{Ti} is the braking tangent forces of a locomotive and cars, kN.

The tangent traction force of a locomotive is determined from formula [13]:

$$T_k=P_{\max}\cdot\varphi_k=\left(L\cdot m\right)\cdot\left(0{,}18+\frac{4}{22+v}\right), \tag{2}$$

where $P_{\max}$ is the maximum traction force of a locomotive, permitted by the conditions of adhesion between the wheels and rails, kN; φ_k is the estimated coefficient of adhesion between the wheels and rails; L is the load from the driving wheelset on rails, kN; m is the number of drive wheelsets of a locomotive equal to the number of traction engines; v is the estimated motion speed, km/h.

The resistance of locomotive motion is determined from [14]:

$$w_l=1.9+0.01\cdot v+0.0003\cdot v^2. \tag{3}$$

The resistance of four-axle cars can be found from:

$$w_c=0.7+\frac{3+0.1\cdot v+0.0025\cdot v^2}{q}, \tag{4}$$

where q is the axial load, kN/axle.

The average braking force per unit weight of the train is determined from:

$$b_B=1000\cdot\vartheta_p\cdot\varphi_{fr}, \tag{5}$$

where ϑ_p is the estimated brake coefficient of a train; φ_{fr} is the estimated coefficient of friction of brake pads.

$$\varphi_{fr}=0.36\cdot\frac{v+150}{2.6\cdot v+150}. \tag{6}$$

According to [15], the cargo car frame strength is calculated as follows:

1) at emergency braking by a pneumatic brake from any speed and at any condition of gaps in automatic coupling devices:

– in a non-uniform train – 2.5 MN;
– in a uniform train – 2.0 MN;

2) at complete service braking to stopping from any motion speed, as well as at controlled braking from a motion speed of 15 km/h and less:

– in a non-uniform train – 2.0 MN;
– in a uniform train – 1.5 MN;

3) at controlled braking from a motion speed over 15 km/h:

– in a non-uniform train – 1.5 MN;
– in a uniform train – 1.2 MN.

To ensure the strength of load-bearing structures in the rolling stock, it is important to study the longitudinal loading and devise measures to ensure traffic safety.

5. Modeling the longitudinal loading on a train equipped with new conceptual couplers

In order to reduce the longitudinal-dynamic efforts in a train under operating modes, including braking, it is proposed to use, instead of a standard automatic coupling device, a conceptual coupler (Fig. 3). In this case, the impact's kinetic energy is damped by transforming it into the work of viscous resistance forces. This resistance is created by moving a viscous liquid through the throttle holes of the piston based on the principle of hydraulic damper operation. The system returns to its original state by using a release spring, which is mounted inside a telescopic element [16].

It is important to note that such a conceptual coupler can be implemented in the rolling stock whose girder beams have a closed cross-section. For example, such a technical solution could be used on cars whose load-bearing elements are made from round pipes.

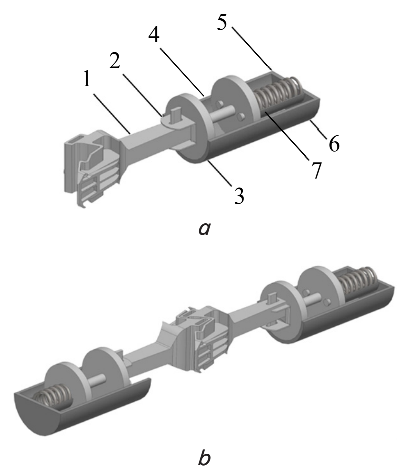

Fig. 3. A conceptual coupler for the automatic coupling: *a* — structural components; *b* — in the interaction between cars; 1 — automatic coupling body; 2 — adapter; 3 — wedge; 4 — girder beam, made from round-section pipe; 5 — bottom; 6 — spring; 7 — telescopic element

To substantiate the use of a conceptual coupler, we performed the calculation using a method for determining the strength of the coupling device through the imaginary separation of a train into two parts. The calculation scheme is shown in Fig. 2.

Suppose that it is required, for the train consisting of 40 cars of model 12-7023, to determine the magnitude and a sign of the reaction between a locomotive and the cars. The locomotive's accepted model is 2TE10V. The speed of the train is 60 km/h.

On the basis of Newton's Law III, the reaction N can be represented in the form of two forces with different signs.

Then the motion equation for the left side of the train takes the form:

$$M_{gw}^{1}\cdot\ddot{x}=\sum K_1\cdot\varphi_{fr}-N-\sum\beta\cdot\dot{x}, \tag{7}$$

for the right part:

$$M_{gw}^{2}\cdot\ddot{x}=\sum K_2\cdot\varphi_{fr}+N-\sum\beta\cdot\dot{x}, \tag{8}$$

where ΣK_1, ΣK_2 are, accordingly, the sum of the forces of pressing the brake pads in the left and right parts of the train, kN; β is the coefficient of viscous resistance, which is created by the conceptual coupler, kN·s/m.

The sum of forces of pressing the brake pads can be found from formula [11]:

$$\sum K=M_{gw}\cdot g\cdot\delta, \tag{9}$$

where δ is the normative value for a coefficient of brake pressing force.

The differential equations (7), (8) were solved by the Runge-Kutta method in the Mathcad programming suite [17–20].

For the left part of the train:

$$Q_1=\begin{bmatrix}\dot{x}\\ \dfrac{\sum K_1\cdot\varphi_{fr}-N-\sum\beta\cdot\dot{x}}{M_{gw}^{1}}\end{bmatrix}, \tag{10}$$

$$X_1=rkfixed\left(Y0,\ tn,\ tk,\ n',\ Q_1\right).$$

For the right part of the train:

$$Q_2=\begin{bmatrix}\dot{x}\\ \dfrac{\sum K_2\cdot\varphi_{k}+N-\sum\beta\cdot\dot{x}}{M_{gw}^{2}}\end{bmatrix}, \tag{11}$$

$$X_2=rkfixed\left(Y0,\ tn,\ tk,\ n',\ Q_2\right).$$

The transition from the systems of second-order differential equations to the first-order differential equations was performed in order to apply the standard algorithms for system solving using the Mathcad rkfixed function.

To solve equations (7) and (8), we used the standard function *rkfixed*($Y0$, tn, tk, n', Q). The $Y0$ vector contains the initial conditions (12). The magnitudes tn and tk determine the starting and final variable of the integration, n' is the fixed number of steps, Q is a symbol vector [21–25]. The models (7) and (8) do not take into consideration the rigidity of release springs, which would also resist the movement of the pistons (Fig. 3).

$$Y0=\begin{pmatrix}0\\0\end{pmatrix}. \tag{12}$$

That is, the initial displacement and speed are equal to zero.

The sum of the forces of pressing the brake pads can be found from formula [11]:

$$\sum K=M_{gw}\cdot g\cdot\delta, \tag{13}$$

where δ is the normative value for a coefficient of brake pressing force.

Under a standard scheme of interaction between a locomotive and the cars, the acceleration operating on the cars was about 1.2 m/s^2 (Fig. 4). Taking into consideration the coefficient of viscous resistance, created by the conceptual coupler, the acceleration was about 0.8 m/s^2. The results were derived for the estimated scheme shown in Fig. 2 and under the input parameters specified above.

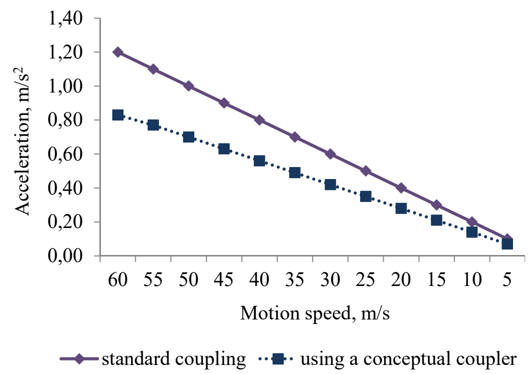

Fig. 4. Accelerations acting on a moving train

In other words, the use of a conceptual coupler makes it possible to reduce the longitudinal loading on a train by almost 30 % compared to the interaction scheme involving the automatic coupling devices SA-3.

6. Calculation of the coupling rod strength

Given that the rod under operating modes perceives significant loads, we calculate its strength.

It should be noted that a given conceptual coupler is proposed instead of the automatic coupling SA-3, whose main component is the absorbing device placed in a traction clamp. It is known that the absorbing device is designed to perceive and mitigate the impacts and jerks in the transmission of compressing and stretching efforts through a car frame (the longitudinal loads) [26]. Therefore, when calculating the rod of the proposed device, we considered the longitudinal loading that occurs under operational modes.

The estimated scheme of a rod will be considered in the form of a pivot system, as a beam with a cantilever clamping (Fig. 5). It is taken into account that the rod receives the load from the piston. A second piston is considered in the form of a rigid clamping. That is, the limitation of a given problem is the absence of piston movement when the rod is loaded. Such a scheme may occur in the case when the rigidity of the release spring of the device exceeds the magnitude of the longitudinal load acting on the rod. In addition, this scheme is valid for the case when the adapter is in an extreme position (in the region of the bottom).

In this case, the maximum stress that operates on the rod would be determined as the sum of stresses arising from effort P_1 (the compression deformation) and P_2 (the bending deformation) [27–29].

The diagram of the transverse force at compression deformation is shown in Fig. 6, *a*); and the diagram of the bending momentum at bending deformation is shown in Fig. 6, *b*).

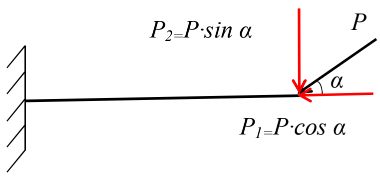

Fig. 5. The rod estimation scheme under the action of angular loads on it

Then, the maximum stresses operating on the rod will be determined from:

$$\sigma_{\max} = \frac{P_1}{A} + \frac{P_2 \cdot l}{W}, \tag{14}$$

where A is the cross-sectional area of the rod, m^2; l is the rod length, m; W is the resistance momentum of the rod cross-section, m^3.

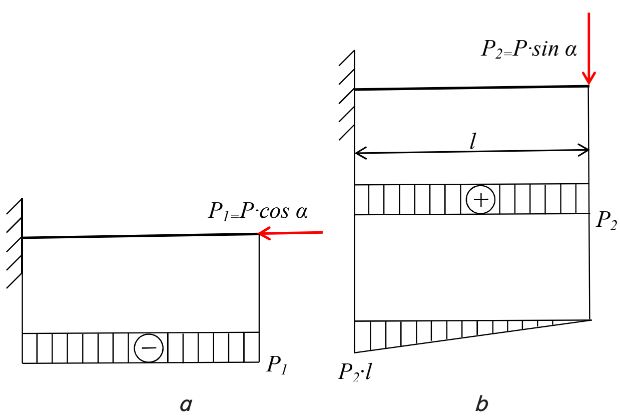

Fig. 6. Results of calculating the rod of a conceptual coupler: *a* — diagram of transverse force; *b* — diagram of bending momentum

Since the component P_1 determines resistance against the longitudinal bending, we checked the following:

$$\sigma_{P_1} = \frac{P_1}{A} \le \frac{\sigma_{cr}}{n_y}, \tag{15}$$

where σ_{cr} is the critical load, MPa; n_y is the resistance reserve.

The piston with the rod was made from steel of brand 09G2S. The value of the yield strength is σ_y=345 MPa and durability limit is σ_d=490 MPa.

It was established that at value P_1=1.2 MH, the rod diameter of 80 mm, the value σ_v=345 MPa and n_c=1, the condition (15) is met.

The rod strength condition in this case takes the form [30, 31]:

$$\sigma_{\max} \le [\sigma], \tag{16}$$

where [σ] are the permissible stresses, MPa.

The following formula is used to determine the transverse angle of the inclination of the automatic coupling axis from the car axle.

$$\alpha=\beta+\gamma, \tag{17}$$

where

$$\beta = \operatorname{arctg}\frac{\ell + c_a + a_l}{R}, \tag{18}$$

$$\beta' = \operatorname{arctg}\frac{\ell' + c'_a + a_l}{R}, \tag{19}$$

$$\gamma = \arcsin\frac{b + b' + \xi}{2a_l}, \tag{20}$$

where l, l' are the semi-bases of the coupled cars, m; c_a, c'_a is the length of the consoles of the coupled cars from the axis of the hoop to the hinge axis of the automatic coupling shank, m; a_l is the length of the automatic coupling body from the center of the hinge shank to the coupling axis, m.

$$b = \frac{(2\ell + c_a)\cdot c_a - \ell_c^2 - a_l^2}{2R}, \tag{21}$$

$$b' = \frac{(2\ell' + c'_a)\cdot c'_a - (\ell'_c)^2 - a_l^2}{2R}, \tag{22}$$

where $2l_c$, $2\ell'_c$ are the bases of bogies of the coupled cars, m; ξ is the additional reciprocal deviation of the automatic coupling hinges in the transverse direction, mm, determined according to [30, 31]; R is the estimated curve radius, m.

It is taken into consideration that a car fits the curve with a radius of R=60 m. In this case, we derived the value of β=6.9 degrees and γ=12.7 degrees. Hence, α=19.6 degrees.

Taking into consideration the above calculations, we obtained σ_{max}=308.1 MPa (a rod diameter of 80 mm and its length is 360 mm), that is the resulting stresses are smaller than those acceptable by 10 %, which are indicated for the operating conditions of cars on various railroad networks for cars' metallic structures [30–32]. Consequently, the strength of the rod is ensured.

We also determined the strength of the rod of our conceptual coupler using a finite element method. The spatial model of the adapter was constructed, whose part is the rod (Fig. 7, *a*). The graphical study was carried out in the SolidWorks software package. The calculation was implemented in the CosmosWorks programming environment. The finite element model of the adapter is shown in Fig. 7, *b*.

The isoparametric tetrahedrons were used as finite elements. The number of nodes of the finite element model was 3,792, elements – 15,554. The maximum size of the element in the model is 30.8 mm, the minimum is 6.16 mm. The percentage of elements with a side ratio of less than three is 96.9, exceeding ten – 0.03.

The load applied to the adapter was taken equal to N=1.2 MN (Fig. 7, *b*). The structure's material is steel, grade 09G2S. The calculation results are shown in Fig. 8.

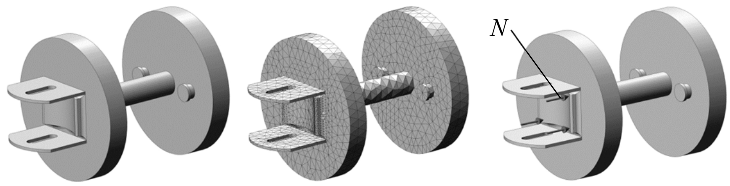

a *b* *c*

Fig. 7. Adapter of a conceptual coupler: *a* – spatial model; *b* – finite-element model; *c* – estimation scheme

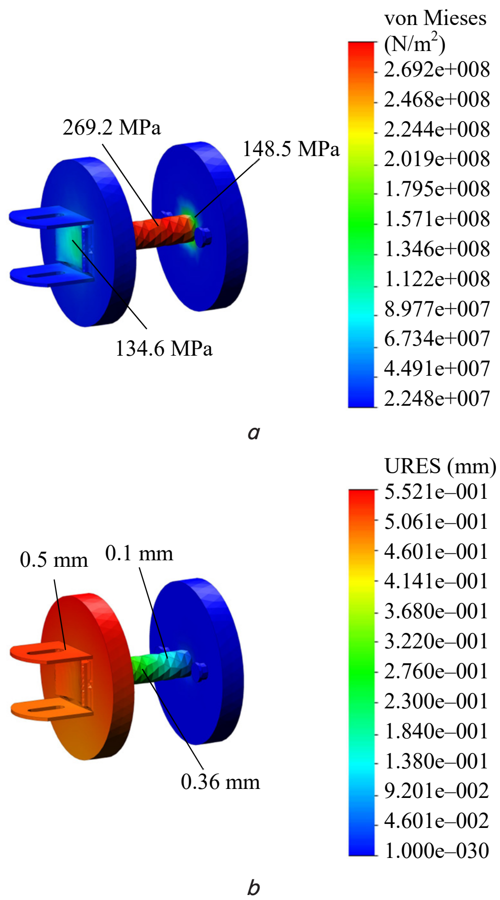

Fig. 8. Results of calculating the strength of the adapter in a conceptual coupler: *a* – stressed state; *b* – displacements in nodes

The maximum equivalent stresses in the adapter are 269.2 MPa, the displacement is 0.5 mm. The maximum deformations amounted to $1.16 \cdot 10^{-3}$. Thus, the strength of the adapter is ensured.

7. Discussion of results of modeling the longitudinal load on rolling stock equipped with the new conceptual couplers

To reduce the longitudinal-dynamic load on a train under operational loads, it is proposed to use a new conceptual coupler instead of the coupling, which is part of the automatic coupling SA-3. A feature of the concept is that the impact's kinetic energy is damped by transforming it into the work of viscous resistance forces (Fig. 3). We have modeled the longitudinal dynamics of the train equipped with the proposed conceptual coupler. It is assumed that the train is uniform, that is, it consists of similar cars.

It was established that the use of the conceptual coupler makes it possible to reduce the longitudinal loading on a train by almost 30 % compared to the interaction scheme involving the automatic coupling devices SA-3 (Fig. 4). This is explained by the fact that the proposed concept generates a viscous resistance to the movement, rather than the elastic-friction as is the case with the automatic coupling SA-3.

The proposed technical solutions would reduce the dynamic loading of cars under load operating modes. This could decrease the amount of damage to cars in operation. In addition, our research results would contribute to the construction of modern rolling stock structures.

To ensure the rod strength of the coupling, we performed the calculation described in the main part of this paper. This takes into consideration the longitudinal load, which acts on the rod (Fig. 5), as the principal one. It was determined that given the accepted geometric dimensions and numerical values of loads, the rod strength is provided (Fig. 8).

It is important to note that modeling the longitudinal dynamics and rod strength of the coupling device was carried out for the case of steady train motion and taking into consideration that the components of the coupling device were made from steel of grade 09G2S. It was taken into consideration that the longitudinal load that a coupling is exposed to is 1.2 MN, which is valid for a uniform train.

In the future, it is necessary to take into consideration the case when a train moves along a broken profile, as well as the transient processes in a train that pulls off and under the action of impact loads. As regards further studies, it also important to determine the influence of the longitudinal dynamics of tank cars with bulk cargo on the operation of a coupling device.

9. Conclusions

1. A mathematical model has been constructed to determine the longitudinal load on a railroad train equipped with the new conceptual couplers. We have determined the maximum loads operating on a train under operational modes. A given model could be used to model the longitudinal dynamics of non-uniform freight trains.

It was established that the proposed device makes it possible to reduce the longitudinal load on a train by almost 30 % compared to the interaction scheme involving the automatic coupling devices SA-3.

2. The rod strength of the coupler has been estimated. The rod estimation scheme was adopted in the form of a pivot system. In this case, the maximum stress, which acts on the rod, was determined by taking into consideration the effect exerted on it by the longitudinal load of 1.2 MN.

Taking into consideration our calculations, at the angle of the lateral deviation of the longitudinal axis of the automatic coupling from the axel of the car α=19.6 degrees, we obtained σ_{max}=308.1 MPa. That is, the resulting stresses are smaller than the permissible ones by 10 %. It was taken into consideration that the structure's material was the steel of grade 09G2S.

We have also determined the strength of the coupling device's rod using the method of finite elements. It was taken into account that the adapter, whose part is the rod, is made of steel of grade 09G2S. The maximum equivalent stresses in the adapter were 269.2 MPa, the displacement is 0.5 mm. The maximum deformations are $1.16 \cdot 10^{-3}$.

Acknowledgments

The present study was conducted within the framework of the scientific topic of young scientists "Innovative principles of creation of resource-saving structures of railroad cars by taking into account the refined dynamic loads and functional-adaptive flash concepts", which is funded by the state budget of Ukraine in 2020.

References

1. Ursulyak, L. V., Shvets, A. O. (2017). Improvement of mathematical models for estimation of train dynamics. Science and Transport Progress. Bulletin of Dnipropetrovsk National University of Railway Transport, 6 (72), 70–82. doi: https://doi.org/10.15802/stp2017/118002
2. Ravlyuk, V., Ravliuk, M., Hrebeniuk, V., Bondarenko, V. (2019). Process features and parametric assessment of the emergence of the excessive wear for the brake pads of freight car bogies. IOP Conference Series: Materials Science and Engineering, 708, 012025. doi: https://doi.org/10.1088/1757-899x/708/1/012025
3. Rakshit, U., Malakar, B., Roy, B. K. (2018). Study on Longitudinal Forces of a Freight Train for Different Types of Wagon Connectors. IFAC-PapersOnLine, 51 (1), 283–288. doi: https://doi.org/10.1016/j.ifacol.2018.05.074
4. Serajian, R., Mohammadi, S., Nasr, A. (2018). Influence of train length on in-train longitudinal forces during brake application. Vehicle System Dynamics, 57 (2), 192–206. doi: https://doi.org/10.1080/00423114.2018.1456667
5. Davydov, Y., Keyno, M. (2016). Longitudinal Dynamics in Connected Trains. Procedia Engineering, 165, 1490–1495. doi: https://doi.org/10.1016/j.proeng.2016.11.884
6. Crăciun, C. I., Cruceanu, C. (2018). Longitudinal dynamic force distribution for different hysteretic buffer characteristics. IOP Conference Series: Materials Science and Engineering, 444, 042003. doi: https://doi.org/10.1088/1757-899x/444/4/042003
7. Crăciun, C., Dumitriu, M., Cruceanu, C. (2017). Parametric study of the distribution of longitudinal dynamic forces developed in the train body using hysteretic characteristics of Ringfeder buffers. MATEC Web of Conferences, 112, 07011. doi: https://doi.org/10.1051/matecconf/201711207011
8. Sharma, S. K. (2018). Multibody analysis of longitudinal train dynamics on the passenger ride performance due to brake application. Proceedings of the Institution of Mechanical Engineers, Part K: Journal of Multi-Body Dynamics, 233 (2), 266–279. doi: https://doi.org/10.1177/1464419318788775
9. Petrenko, V. (2016). Simulation of Railway Vehicle Dynamics in Universal Mechanism Software. Procedia Engineering, 134, 23–29. doi: https://doi.org/10.1016/j.proeng.2016.01.033
10. Wu, Q., Spiryagin, M., Cole, C. (2016). Longitudinal train dynamics: an overview. Vehicle System Dynamics, 54 (12), 1688–1714. doi: https://doi.org/10.1080/00423114.2016.1228988
11. Kazarinov, V. M. (1981). Avtotormoza. Moscow, 464.
12. Vershinskiy, S. V., Danilov, V. N., Husidov, V. D. (1991). Dinamika vagona. Moscow, 360.
13. Babichkov, L. M., Gurskiy, P. A., Novikov, L. P. (1971). Tyaga poezdov i tyagovye raschety. Moscow, 280.
14. Asadchenko, V. R. (2004). Raschet pnevmaticheskih tormozov zheleznodorozhnogo podvizhnogo sostava. Moscow, 120.
15. Babaiev, A. M., Dmytriev, D. V. (2007). Pryntsyp diyi, rozrakhunky ta osnovy ekspluatatsiyi halm rukhomoho skladu zaliznyts. Kyiv, 176.
16. Fomin, O., Lovska, A., Masliyev, V., Tsymbaliuk, A., Burlutski, O. (2019). Determining strength indicators for the bearing structure of a covered wagon's body made from round pipes when transported by a railroad ferry. Eastern-European Journal of Enterprise Technologies, 1 (7 (97)), 33–40. doi: https://doi.org/10.15587/1729-4061.2019.154282
17. Plakhtii, O., Nerubatskyi, V., Ryshchenko, I., Zinchenko, O., Tykhonravov, S., Hordiienko, D. (2019). Determining additional power losses in the electricity supply systems due to current's higher harmonics. Eastern-European Journal of Enterprise Technologies, 1 (8 (97)), 6–13. doi: https://doi.org/10.15587/1729-4061.2019.155672
18. Fomin, O. (2015). Improvement of upper bundling of side wall of gondola cars of 12-9745 model. Metallurgical and Mining Industry, 1, 45–48.
19. Lovskaya, A. (2015). Computer simulation of wagon body bearing structure dynamics during transportation by train ferry. Eastern-European Journal of Enterprise Technologies, 3 (7 (75)), 9–14. doi: https://doi.org/10.15587/1729-4061.2015.43749
20. Kondratiev, A. V., Gaidachuk, V. E., Kharchenko, M. E. (2019). Relationships Between the Ultimate Strengths of Polymer Composites in Static Bending, Compression, and Tension. Mechanics of Composite Materials, 55 (2), 259–266. doi: https://doi.org/10.1007/s11029-019-09808-x
21. Kelrykh, M., Fomin, O. (2014). Perspective directions of planning carrying systems of gondolas. Metallurgical and Mining Industry, 6, 64–67.

22. Lovska, A. (2018). Simulation of Loads on the Carrying Structure of an Articulated Flat Car in Combined Transportation. International Journal of Engineering & Technology, 7 (4.3), 140. doi: https://doi.org/10.14419/ijet.v7i4.3.19724
23. Fomin, O., Gerlici, J., Lovska, A., Kravchenko, K., Prokopenko, P., Fomina, A., Hauser, V. (2019). Durability Determination of the Bearing Structure of an Open Freight Wagon Body Made of Round Pipes during its Transportation on the Railway Ferry. Communications - Scientific Letters of the University of Zilina, 21 (1), 28–34.
24. Kučera, P., Píštěk, V. (2017). Testing of the mechatronic robotic system of the differential lock control on a truck. International Journal of Advanced Robotic Systems, 14 (5), 172988141773689. doi: https://doi.org/10.1177/1729881417736897
25. Pistek, V., Klimes, L., Mauder, T., Kucera, P. (2017). Optimal design of structure in rheological models: an automotive application to dampers with high viscosity silicone fluids. Journal of Vibroengineering, 19 (6), 4459–4470. doi: https://doi.org/10.21595/jve.2017.18348
26. Lukin, V. V., Shadur, L. A., Koturanov, V. I., Hohlov, A. A., Anisimov, P. S. (2000). Konstruirovanie i raschet vagonov. Moscow, 731.
27. Vatulia, G., Falendysh, A., Orel, Y., Pavliuchenkov, M. (2017). Structural Improvements in a Tank Wagon with Modern Software Packages. Procedia Engineering, 187, 301–307. doi: https://doi.org/10.1016/j.proeng.2017.04.379
28. Molotnikov, V. Ya. (2017). Tehnicheskaya mehanika. Sankt-Peterburg, 476.
29. Filatov, Yu. E. (2017). Vvedenie v mehaniku materialov i konstruktsiy. Sankt-Peterburg, 320.
30. DSTU 7598:2014. Vaho ny vantazhni. Zahalni vymohy do rozrakhunkiv ta proektuvannia novykh i modernizovanykh vahoniv koliyi 1520 mm (nesamokhidnykh) (2015). Kyiv, 162.
31. GOST 33211-2014. Vagony gruzovye. Trebovaniya k prochnosti i dinamicheskim kachestvam (2016). Moscow, 54.
32. BS EN 12663-2. Railway applications. Structural requirements of railway vehicle bodies. Freight wagons (2010). British Standards Document. doi: https://doi.org/10.3403/30152552u

UDC 629.7.035.7
DOI: 10.15587/1729-4061.2020.199486

A NUMERICAL STUDY OF PERFORMANCE OF THE SMALL-SIZE UAV PUSHING TANDEM PROPELLER WITH JOINED BLADES

M. Kulyk
Doctor of Technical Sciences, Professor, Head of Department*
F. Kirchu
PhD, Associate Professor*
E-mail: fkirchu@gmail.com
Hussein Hanesh
Postgraduate Student*
*Department of Aviation Engines
National Aviation University
Liubomyra Huzara ave., 1,
Kyiv, Ukraine, 03058

Розроблена нова форма тандемної лопаті з вдосконаленим розташуванням профілів по відношенню до відомих гвинтів, в яких профілі розташовуються подібно до тандемного крила літака. Запропоновано нове розташування профілів по висоті лопаті. За основу для проектування було взяте розташування профілів подібне до тандемних лопаткових вінців компресорів та вентиляторів. Такий підхід дозволив ліквідувати аеродинамічне затінення лопатей та підвищити їхню аеродинамічну навантаженність. Для об'єднання лопатей в кінцевій частині застосована спіралеподібна перетинка, яка дозволила значно знизити кінцеві вторинні втрати за рахунок запобігання утворення кінцевого вихору.

Для дослідження характеристик тандемних гвинтів та структури газодинамічної течії навколо них розроблена розрахункова модель гвинта в періодичній постановці, що дозволило значно скоротити час розрахунку. Моделювання здійснювалось в програмному комплексі ANSYS CFX, в якому реалізований алгоритм вирішення нестаціонарних осереднених по Рейнольдсу рівнянь Нав'є-Стокса замкнутих моделлю турбулентності SST Ментера. В результаті моделювання отримані характеристики тандемного гвинта, які підтвердили правильність вибраного підходу щодо проектування тандемної лопаті. ККД розробленого гвинта досягає рівня 75 % на розрахунковому режимі, що є дуже хорошим показником для малорозмірних гвинтів, які працюють при низьких значеннях числа Рейнольдса. Для порівняння, ККД класичних, подібних по геометричним характеристикам гвинтів, знаходиться в межах 50–60 %. При використанні тандемного гвинта з об'єднаними лопатями як штовхаючого рушія відзначено зниження його тяги на рівні 3–4 %, що обумовлено утворенням зони розрідження у втулковій частині та в області кока

Ключові слова: повітряний гвинт, кінцевий вихор, стрічка Мьобіуса, коробчатий гвинт, тандемний гвинт

Received date 22.01.2020
Accepted date 20.03.2020
Published date 24.04.2020

1. Introduction

The propeller, as a thruster, has been known for a very long time and has been the only possible mover in aviation for many years. The increase in flight speed, the emergence of jet, and then turbofan gas turbine engines significantly reduced the use of propellers. However, it should be noted that today the propeller has no competitors in terms of profitability at moderate flight speeds ($M \leq 0.6$, and in the case of coaxial counter-rotating fans, $M \leq 0.8$). Also, propellers